ACCURATE CHARACTERISATION OF SURFACE FATIGUE CRACKS (IN STEELS) USING THE AC POTENTIAL DROP NDT TECHNIQUE

R.B. Tait, D. Bright*, & J.F.W. Bell***

* Department of Electrical Engineering, University of Cape Town

** Department of Mechanical Engineering, University of Cape Town

Abstract: An ACPD method has been developed as an NDT technique that can accurately characterize surface breaking fatigue cracks in metal specimens. Single fatigue cracks that were initiated and propagated in different specimens were considered. The factors investigated were the sensitivity of the apparatus, skew cracks, load effects, closure effects and cracks of different flaw shapes (or aspect ratios). The results obtained demonstrate that the present method could accurately characterise a fatigue crack in terms of its depth, shape and orientation.

INTRODUCTION

Background

In order to maintain the desired level of safety in an industrial environment, it is important that the structural integrity of all the components and equipment being utilised by the facility is assured. The flaws present in a structure can be assessed by a "fitness-for-purpose" Fracture Mechanics approach, which requires that all the defects be below a maximum specified size in order for the structure to function at the required level of safety for the necessary length of time. The fracture mechanics perspective assesses the interrelationship between the size of an inherent flaw, a, in a structure, in conjunction with the stresses the system sustains, σ, to a local stress intensity, K. When K exceeds the local material's resistance to cracking, or its "fracture toughness", K_{IC}, fast, brittle failure is imminent, i.e.

$$Y\sigma\sqrt{(\pi a)} = K \qquad \text{(stress intensity)} \qquad (1)$$

and, when $K \geq K_{IC}$ failure occurs.

In addition, equation (1) also includes a compliance function *Y*, which is dimensionless and takes into account the shape of the flaw as well as the relative dimensions of the component in which the flaw is located. From this expression, it is clear that the flaw size is critical in determining whether a material will fail under an applied load. This interrelationship between the stress, flaw size and material toughness is sometimes referred to as the "triangle of integrity".

To determine the structural integrity of an engineering system precisely using equation (1), not only must the depth of the flaw, *a*, be established, but the crack profile must also be obtained in order to assess the extent of the crack, as shown in Figure 1. That is, the aspect ratio (crack depth to crack surface length, *a / 2c*) must be obtained, thus enabling determination of the *Y* function, and facilitating the "fitness-for-purpose" assessment.

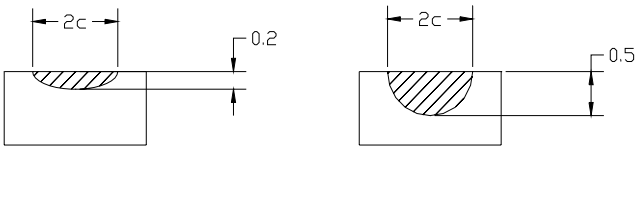

Fig 1 Thumbnail cracks with identical surface lengths (2c), but different aspect ratios

Many NDT procedures do not necessarily give an accurate characterisation of the crack in a material [1-4]. Optical and surface methods such as dye penetrant and magnetic particle inspection (MPI), although convenient for crack detection, do not provide crack depth readings. X-Ray methods can detect globular type flaws, but are not suitable for

tight fatigue cracks. Eddy current testing is reliable for crack detection, but is not accurate in sizing. Ultrasonic pulse-echo (PE) approaches, although widely used, have a relatively large sizing error (typically ± 5mm) and even time-of–flight diffraction (TOFD), although a lot more accurate (± 0.4mm), is very labour intensive as the testing procedure can be tedious, and accuracy can only be provided at great expense. The potential drop (PD) technique, however, has been used previously as a research tool in flaw characterisation, and has achieved good accuracy [5-16]. The present work described in this paper discusses the development of an ACPD system as an NDT technique for flaw detection and sizing of variously shaped and oriented surface breaking fatigue cracks.

Theory

The principle of the ACPD method lies in Ohm's Law, where a conductor carrying a current will exhibit a resistance. This resistance is proportional to the potential drop (PD) measured across the conductor, and is a function of specimen material, environmental effects (such as temperature), and length of the current path. Thus, if the length of the current path is altered by a crack in the conductor, there will be a proportional increase in the potential drop.

AC current flowing in a conductor flows in a thin region at the surface of the conductor as described by Maxwell's equations. This depth of penetration of the current δ, known as the "skin depth", is inversely proportional to the square root of the current frequency f, the conductivity σ, and permeability μ of the conductor, and can be given as

$$\delta = (\pi f \sigma \mu)^{-1/2} \qquad (2)$$

Reducing the skin depth has been found to increase the sensitivity of the ACPD system [5]. Previous research has also shown that the relationship between crack depth and voltage drop is somewhat nonlinear [6]. In theory, however, this relationship should be nominally linear, as the change in resistance in an infinite, completely elastic metal

specimen including a surface crack, is linear. The PD measured across a crack, however, is not only a function of the current path. Studies conducted on the ACPD device have revealed that the output of the ACPD system is dependent on other factors, including: input current magnitude and frequency, loading history and material plasticity, crack closure, electromagnetic effects, edge effects, temperature and voltage probe configuration [5-16]. In order to develop an accurate crack characterization system, all of the features of this technique must be examined.

The total output of the ACPD system V_{out} , measured under a constant applied load, can therefore be given as

$$V_{out} = V_{specimen} + V_{coil} + V_{magnetostrictive} + V_{plastic} - V_{closure} \quad (3)$$

where, $V_{specimen}$ is the voltage induced as a result of the material properties, the crack length, the temperature and the applied current [9],
V_{coil} is the voltage induced in the voltage probe leads as a result of their relative positions, and is of an inductive nature, proportional to the input current frequency [5,10,15,16],
$V_{magnetostrictive}$ is the voltage created by a load applied to a specimen, and is dependent on the state of strain of the material [5,8,9,13],
$V_{plastic}$ is the voltage caused by the current flowing through a region of a specimen where the material has gone plastic, and possibly work hardened [7,9,11],
and $V_{closure}$ is the reduction in the voltage caused by current flowing across the crack as a result of crack closure [12,13].

Load Effects

Applying a stress to the material causes a change in its magnetic state, and is known as the Villari effect or inverse magnetostriction [5,9]. The Villari effect may be prevalent in the ACPD system. Thus, when a test specimen undergoes loading, the magnetic state of the material can experience a change, which will change the magnetic field generated

around the specimen as a result of the flow of current. This will cause the current flow to change, and thus a change in the measured potential can occur.

Electrostriction is a phenomenon present in most materials. It can be defined as the dimensional change of a conducting material caused by a change in the state of its electric field as a result of an applied electric field [17]. If a material is placed under a stress, and a strain results, an electric field is also created, and thus a voltage is produced. The magnitude of the strain is dependent on the square of the magnitude of the electric field.

Crack closure is associated with fatigue cracking as a result of the formation of a plastic zone at the stress concentration at the crack tip while the fatigue crack is propagating. When a cracked specimen is unloaded, residual stresses remain as a result of this plastic zone, and act in compression across plastic asperities of the crack wake. Current conduction can occur across the crack through a short-circuit conduction path across the asperities. Previous studies have shown conflicting results as to the extent of current flowing across the crack as a result of the crack faces being forced together [12,13].

EXPERIMENTAL DETAILS

In the present case, PD characteristics were investigated by passing a current through various conducting metal specimens in which cracks could be introduced, and measuring the PD across any such defect, and in the nearby vicinity. The associated equipment, discussed below, facilitated this procedure.

In this study, a dual voltage probe system was adopted, which compared the voltage across the crack to some reference voltage measured away from the crack. This system eliminates thermoelectric and other temperature effects, and maintains the positions of the probe leads constant, thereby eliminating the effect of V_{coil}, as it remained constant as the positions of the probe leads was maintained. It is also important to note that the loading applied to the specimens was low enough not to generate a significantly large

plastic region in the specimens, and the rate of crack propagation was held constant to maintain a small but constant size plastic zone. Thus, the voltage $V_{plastic}$ remained effectively constant throughout the test sequence, and its effect on the PD resulting from crack extension could therefore be ignored.

Experimental System

A variac and a transformer, connected to mains, supplied the input current of 0.5A at 50Hz. The voltage signals from the specimen passed through an electronic circuit that amplified, filtered and converted the noisy AC signals into clean DC voltages. The output of the circuit was measured by an HP34401A digital multimeter, which was controlled by a PC running different programs written in HP Vee. For every measurement made by the multimeter, ten voltage readings were taken and analysed. From these readings, the mean and standard deviation were calculated so that the accuracy of the ACPD system could also be obtained.

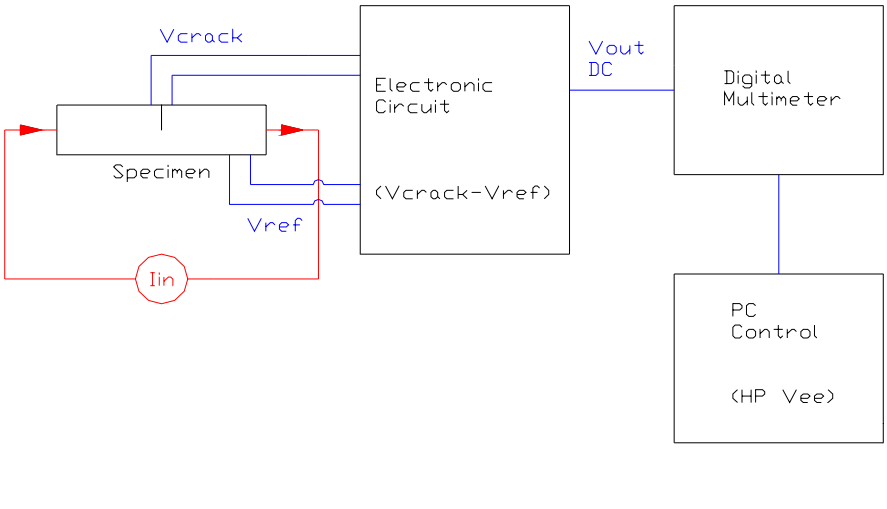

Fig 2 Block Diagram of the ACPD System

Applied Input Current

A mains power supply of 50Hz was adopted for the AC input current, which was converted into a 0.5A current by a transformer. As the signal from mains is notoriously unstable and noisy, a dual voltage probe system was adopted so that a reference voltage could be provided to negate the effects of the unpredictable signal. The use of a 50Hz signal resulted in a skin depth of 0.8mm in steel, and caused less voltage to be induced in the voltage probe leads, as V_{coil} was proportional to the square root of the frequency of the signal. In addition, the use of a relatively low 0.5A current also resulted in a weaker electromagnetic field being generated around the specimen, which lessened the effects that any nearby electrical or magnetic object may have had on the potential drop readings. The low current also did not cause a large temperature increase in the specimen as a result of current flow, and thus any thermoelectric errors that developed were minimal.

Electronic Measurement System

The electronic system presented in this paper evolved as needs for a more accurate and sensitive device was required.

Phase I

The ACPD system was based on a synchronous detection system, but the voltage measured across the crack was divided by the reference voltage, and not multiplied as in a regular synchronous detection system. The reference voltage was the voltage measured on the specimen surface at a distance from the crack, which was amplified and filtered in the same manner as the crack voltage. Thus, dividing the two signals provided a ratio signal, which minimised the effects of the unstable input current. This ratio was then filtered and converted to a DC signal, the so called PD_{ratio}.

Phase II

A more accurate system was realized using a complete dual channel system, where the AC voltage signals across the crack and at some reference point were separately amplified, filtered and converted to DC. These voltages were then measured simultaneously by a digital multimeter, which then performed the division of the signals digitally, which provided a more accurate PD_{ratio}.

Phase III

The final step in the developmental evolution of the PD system was the introduction of an instrumentation amplifier at the output of the dual channel circuit to provide an accurate differential signal by comparing the crack voltage to the reference voltage. Therefore, the output signal, V_{dc}, was a direct indication of the difference in the distance the current traveled between the pairs of probes only, and thus was a direct measure of the resistance, which could be related to the depth of the crack.

Material and Specimen Geometry

Two different materials were used for the preparation of specimens. Mild steel (σ_y = 300MPa, $\rho = 7.0*10^{-8}$ Ωm) was used to fabricate five different types of specimens, and high strength 7075 aluminium (σ_y = 500MPa, $\rho = 2.75*10^{-8}$ Ωm) was used for a singular type of specimen. The first steel type was a 2mm thick sheet metal strip of dimensions 500 by 40mm. The second type was an SENB specimen of dimensions 112 by 24 by 12mm, with a 60^o notch machined 3mm deep (SENB). The third type was a specimen with no notch and dimensions 112 by 24 by 12mm, rather like a conventional modulus of rupture test specimen (MOR). The aluminium specimen type was of dimensions 112 by 24 by 12mm, identical in geometry to the steel MOR specimens.

The fourth type of steel specimen was a specimen 200 by 40 by 8mm, used in evaluating skew saw cuts (SSC) at different angles, which are shown in Figure 3. The last steel

specimen type (Figure 4) was a thumbnail ribbed bending (TRB) specimen of basic dimensions 240 by 50 by 20mm, which included a machined rib of width either 5 or 15mm [18]. This ribbed specimen was pre-fatigued by a load of typically 12kN applied at a frequency of 10Hz until a crack propagated through the rib and into the body of the specimen. The rib was then machined off to provide a smooth surface for inspection, but with the specimen containing an atomically sharp, tight fatigue crack.

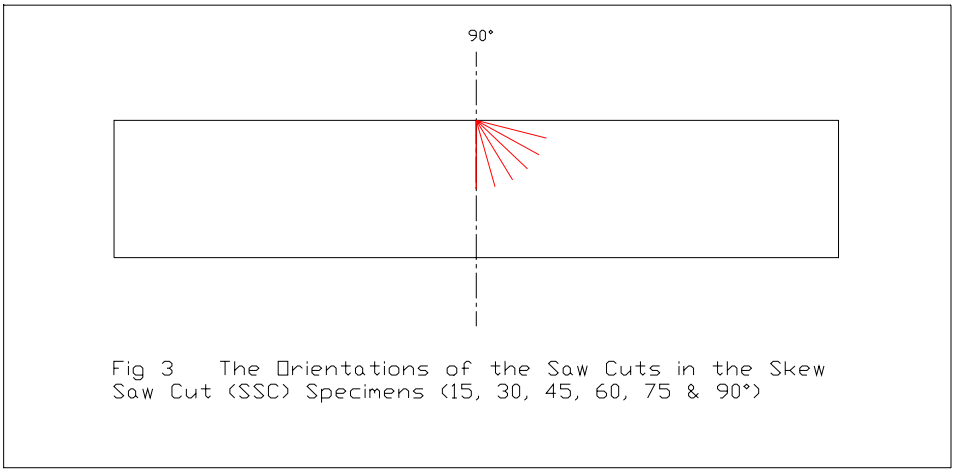

Fig 3 The Orientations of the Saw Cuts in the Skew Saw Cut (SSC) Specimens (15, 30, 45, 60, 75 & 90°)

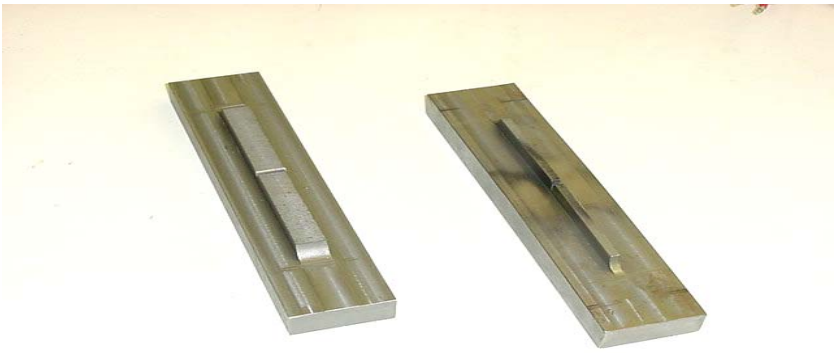

Figure 4 The TRB specimens, displaying the different rib widths. The specimen on the left has a rib of 15mm, and the specimen on the right has a rib 5mm thick. Fatigue cracks were grown through the rib, which was then machined off leaving a tight fatigue crack in the bulk specimen.

Test Matrix

The following tests were conducted in this study:

1. Initial specimens containing saw cuts were investigated to determine the feasibility of the ACPD technique. Fatigue specimens were then loaded in three-point bending by an ESH servo-hydraulic test rig. A sinusoidal load of 11,6kN at 10 Hz with an R-ratio of 0.1 was applied to the SENB specimens. These loads were large enough to initiate and propagate a fatigue crack, but small enough not to introduce a large plastic zone in the specimen. These tests were used to investigate the sensitivity of the apparatus, and its viability for use on fatigue cracks (typical of those encountered in industry), rather than machined slots.

2. Initially, the system developed in Phase I of the ACPD evolution was employed to provide results on a skew crack. A mobile voltage probe system was then used on the SSC specimens using Phase III to provide a profile of the potential drop on both sides of a saw cut. The voltages across the crack and on either side of the crack were examined.

3. To investigate load effects and closure on the PD, specimens were tested in three-point bending from no load to some appropriate maximum, and then in unloading.

4. The pre-fatigued thumbnail cracks, created using the ribbed specimens, were loaded in three-point bending. A sinusoidal load of 12,4kN at 10 Hz with an R-ratio of 0.1 was applied to the TRB specimens. Potential measurements were taken over the crack, and along its surface length, to quantify the effect of different aspect ratios using the ACPD device.

EXPERIMENTAL RESULTS AND DISCUSSION

Sensitivity Test Results

Preliminary tests were conducted on saw cuts in the steel sheet specimens for Phase I. Potential drop readings were obtained for 1mm increments in crack depth. Measurements were taken using a system of probes that were soldered onto the specimen. The sensitivity of the device was not completely satisfactory, but the results that were obtained (Figure 5) provided some insight into the ACPD technique.

Figure 5 Graph of PD_{ratio} vs Saw Cut Crack Length for Phase I

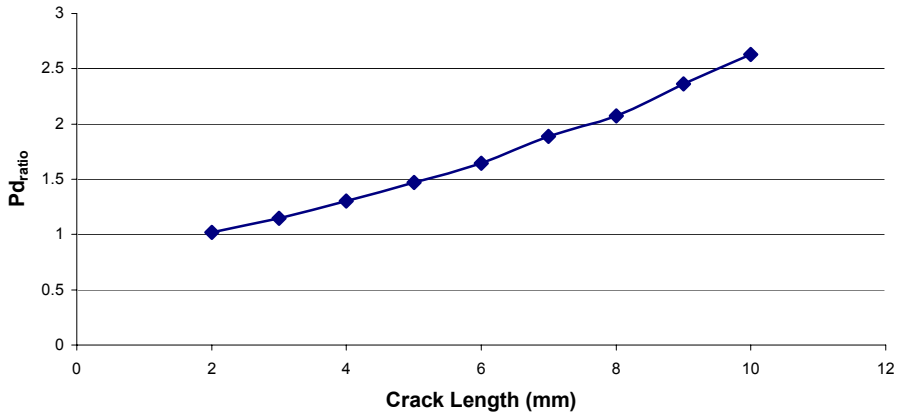

Further tests on fatigue cracks were conducted using the Phase II system. The results that were obtained are displayed in Figure 6. For crack depths smaller than the skin depth, the ACPD device is not very sensitive, as the current can merely flow around the crack without much change in the current path. However, once the crack extends past the skin depth, the sensitivity of the system to an increase in the crack depth was enhanced. From the results, a 0.1 mm change in crack length, gives an average PD ratio change of 6.5 mV. The maximum standard deviation of the readings was determined experimentally to be $2*10^{-3}$, therefore, the sensitivity of the device *S*, in terms of detectable crack length increment, can be calculated to be

$$S = 0.1/(6.5/(2*2)) = 61.5\ \mu m$$

Figure 6 Graph of PD_{ratio} vs Crack Length for Phase II

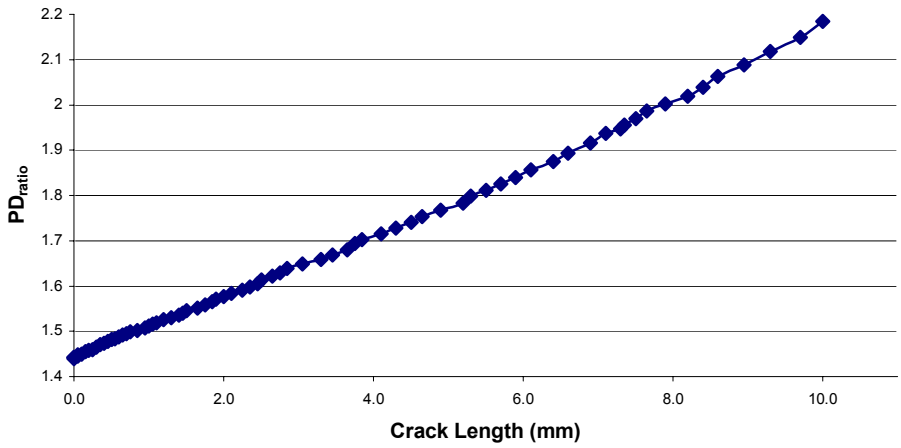

The system developed in Phase III, which provided a differential output, was then used for tests conducted on SENB fatigue specimens. Figure 7 displays the results typical of this system.

Figure 7 Graph of V_{dc} vs Fatigue Crack Length for Phase III

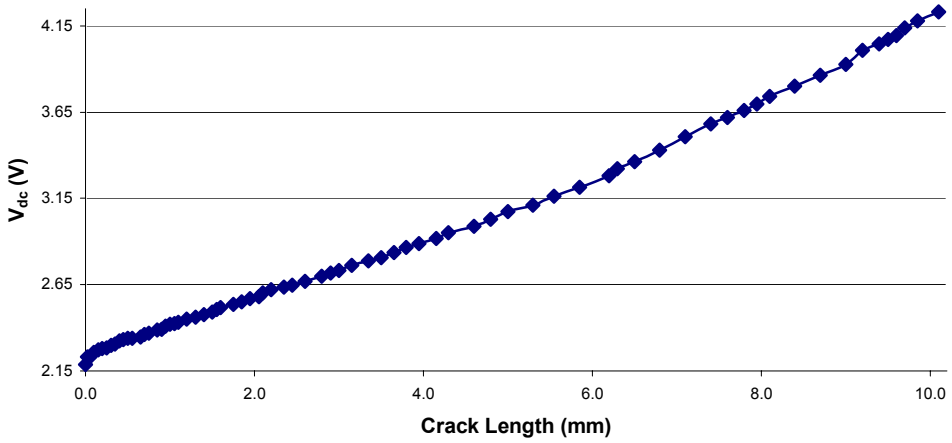

For the Phase III system, a 0.1 mm change in crack length resulted in a V_{dc} change of 10 mV. Now, with a maximum standard deviation of the readings of $2*10^{-3}$, the crack increment sensitivity is calculated as

$$S = 0.1/(10/(2*2)) = 40\ \mu m$$

Thus, the Phase III system is even more sensitive than the previous system.

Skew Crack Results

The PD results for the Phase I system are given below in Figure 8. Voltage readings were taken at 5 mm divisions on both sides of a crack cut at 45^{o} to the specimen surface for 1mm increments of crack growth. The voltage profile of the crack revealed that a skew crack could be readily detected.

Figure 8 Graph of PD_{ratio} vs Position for a Skew Crack Propagated at 45 degrees to the Left for Crack Lengths of 2, 5 & 10mm for Phase I

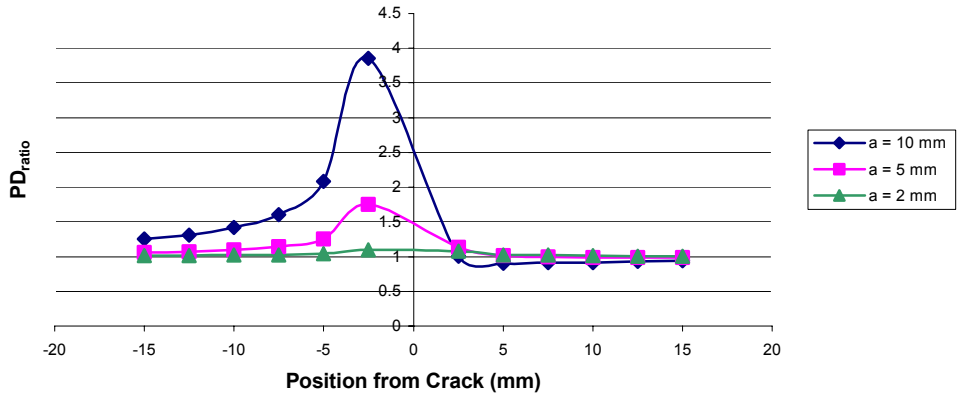

The Phase III system was used to analyse the effect on the measured PD of skew cracks at different angles in steel specimens. The voltage profiles for saw cuts were investigated at 1mm crack increments, while the probe was placed over the crack, initially with the crack positioned in the centre of the probes, then with one of the probes 1mm from the crack, then followed by all subsequent measurements taken at 5mm divisions. This facilitated thorough investigation of the voltage profile due to the skew crack. Figure 9 depicts the results obtained by a crack propagated at 45^{o} crack to the surface of the specimen.

Figure 9 Graph of V_{dc} vs Position for a Crack Orientated at 45 degrees to the Left, for a Crack Length from 0 to 7mm for Phase III

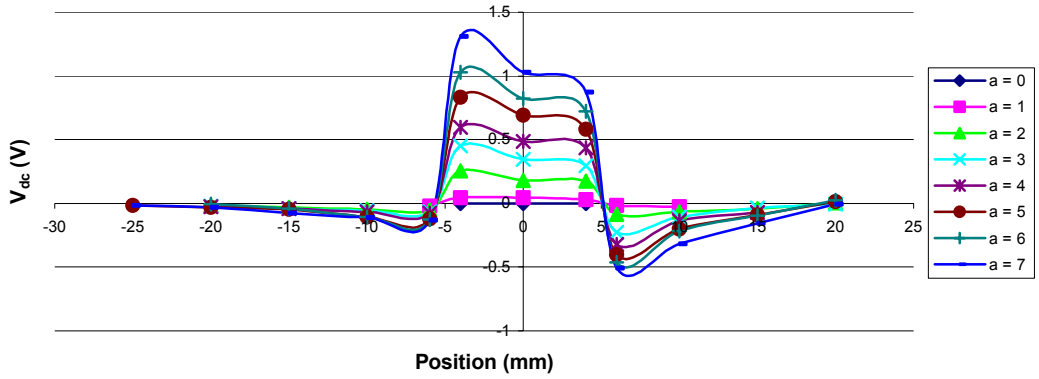

The voltage profile is visibly asymmetric, which lends this system to the detection of crack orientation. Figure 10 depicts the difference in voltage between the potential across the crack on the surface, with the crack at the centre of the probes, and with the probe 1mm from the crack on the cracked side of the specimen. This graph displays the different effects that cracks of different orientations have on the measured potential.

Figure 10 Graph of V_{dc} vs Crack Length for the Cracked Side of the Specimens with Crack Orientations of 15, 30, 45, 60, 75 & 90 degrees

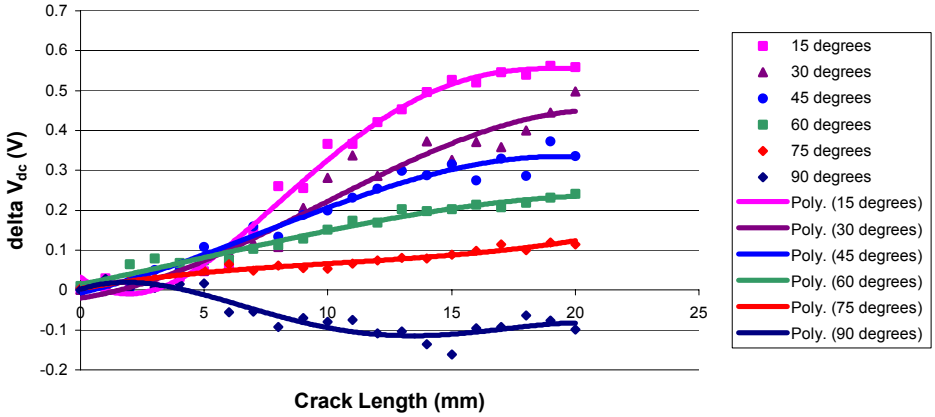

As is evident from the results using the present system, the orientation of a crack less than 5mm deep cannot be accurately detected, but the comparison of the measured voltages for a crack greater than 5mm can be used to reveal the orientation of the crack.

Load Effects

The system of Phase III was used to analyse the effects of bending loading on the test specimens. Initially the voltage of previously cracked SENB specimens from the sensitivity tests was obtained for an increasing constant load. The specimen was then unloaded, and voltage readings were taken for the same loads as in loading. Figure 11 reveals a typical curve of the voltage obtained under different loads.

Figure 11 Graph of V_{dc} vs Load Increasing from 0 to 4kN and then back to 0 load for a Cracked Specimen for Phase III

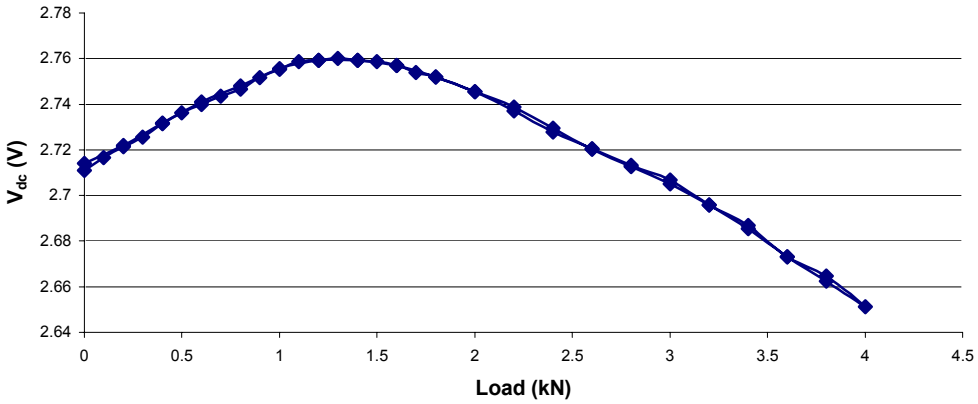

The initial increase in potential can be attributed to crack closure effects, or the opening out of short-circuited asperities initially created by fatigue crack tip plasticity. As the specimen was loaded, the crack faces separated, and so no current could move across the crack, thus increasing the current path, and thus the resistance, which causes a proportional increases in the voltage. At some maximum load, the voltage begins to decrease, and it continues to do so until the maximum allowable load is reached. The increase in the voltage caused by crack closure is approximately 50mV, which will result in the accuracy of the system decreasing to 0.5mm.

Uncracked specimens were then tested in the same manner as the cracked specimens to investigate the effect of load alone on an uncracked specimen, to distinguish if this effect was due to some fatigue crack phenomenon. A typical graph is shown below in Figure 12.

Figure 12 Graph of V_{dc} vs Load Increasing from 0 to 4kN and then back to 0 load for an Uncracked Specimen for Phase III

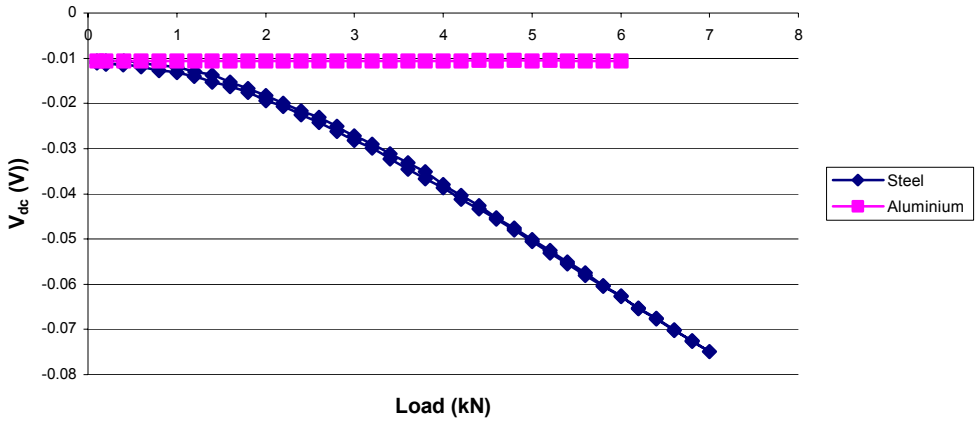

From the graph, it can be observed that for a 7kN load, the voltage measured by the ACPD system decreased by approximately 70mV. Now, for Phase III a 0.1mm change in the crack length will reliably give a measurable increase in the output voltage of 10mV. Thus, if the load effects on the steel specimens are ignored, the accuracy of the system decreases to 0.7mm. The results suggest that this response is caused by some property of the specimen material, and not by a crack effect. Past research suggests that this response of a material to an applied load is caused by a phenomenon known as magnetostriction [5,9,13]. However, in the previous sets of tests, no hysterisis was exhibited by the specimens, and therefore, this effect may be caused by electrostriction rather than magnetostriction [17]. Aluminium MOR specimens were tested under the same loading as the previous tests. It was established that in all the aluminium specimens, negligible change in the voltage across the crack occurred with an increase in the applied stress. Figure 12 also displays the results obtained for the aluminium specimens.

Therefore, this feature of a change of PD with load appears to be caused by the magnetic phenomenon known as magnetostriction, even though it does not exhibit hysterisis. This absence of hysterisis may result from the small-scale change in the magnetization of the specimen following an extremely small hysterisis loop, which was not detected, but the phenomenon warrants further investigation

Crack Shape Effects

Thumbnail fatigue cracks of two different aspect ratios were grown in the TRB specimens. The potential was measured at 2mm divisions over the length of the crack on the surface to provide a profile of the shape of the crack. The PD profiles for two cracks of different aspect ratios, including a photograph of the actual fatigue cracks are shown in Figures 13 and 14. The voltage profile revealed the shape of the crack, although if can be seen from the graph that the potential measurements for a larger crack were higher than expected at positions far from the crack. This was due to edge effects of the specimen, as the current was forced to flow in a decreasing area between the crack and the edge of the specimen.

Figure 13 The voltage profile obtained in (a) is for the thumbnail crack displayed in (b)

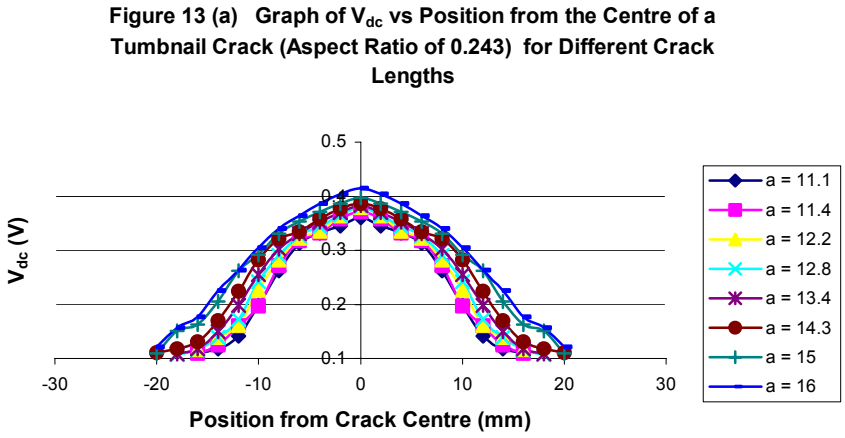

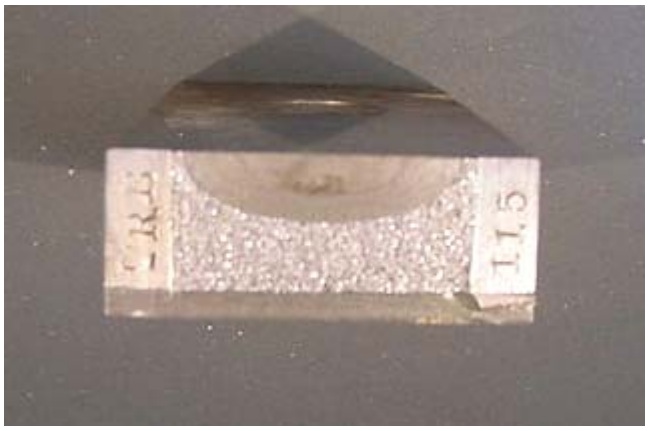

Figure 13 (b) Photograph displaying the actual shape of the thumbnail crack investigated

Figure 14 The voltage profile obtained in (a) is for the thumbnail crack displayed in (b)

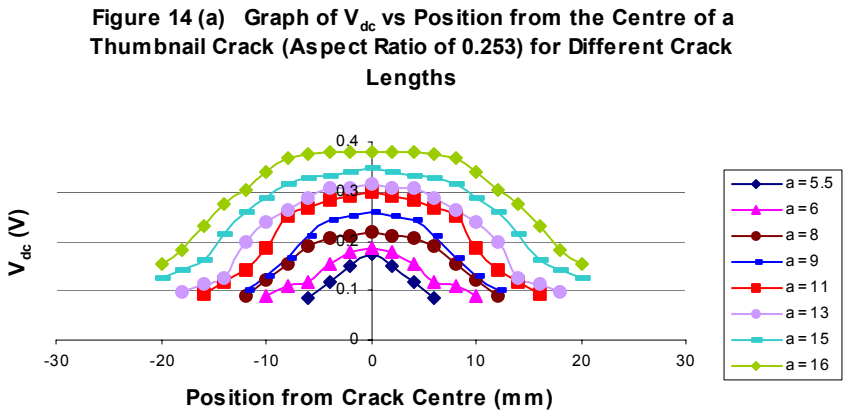

Figure 14 (b) Photograph displaying the actual shape of the thumbnail crack investigated

CONCLUDING REMARKS

An ACPD system has been developed for use as an NDT device for evaluating and sizing fatigue cracking in steel components. In particular fatigue cracking, being sharp and tight, truly represents flaws found in industrial components. The present ACPD system has many advantages over other crack sizing systems, such as remarkably accurate fatigue flaw sizing to 40 microns and the ability to distinguish skew cracks and cracks of variable aspect ratio. In addition, the use of a mains power source makes this system extremely practical. This was achieved by the design of an electronic circuit containing the minimum amount of analog components to process the ACPD signals and to reduce inherent errors. The use of a dual probe voltage measurement system further decreased

the effects of any electrical noise introduced into the system, and resulted in no voltage being induced in the voltage probe leads. The results also showed that crack closure effects affect the measured potential across the crack, and that the potential also decreases with load in ferromagnetic specimens. Both of these effects are small, however, when compared with the potential caused by crack extension, but deserve further investigation. The voltage profiles measured on either side of and along the length of the crack revealed that the discrimination of crack orientation and crack profile are both feasible. Thus, the present ACPD system is seen as a precursor in the development of a device, which can be used as a second-tier NDE tool for accurate crack characterisation.

REFERENCES

[1] R.L. Smith, Recent developments in nondestructive testing, *Nondestructive testing*, 187-191, 1987

[2] M.G. Silk, Weld inspection methods, *Metals and Materials*, 192-196, 1989

[3] J.R. Lilley & C.D. Perrie, Developments in NDT, AEA Technology, 1997

[4] C.A. Lamy, J.M.A. Rebello, A. Sauer & J. Carlier, Surface crack sizing related to the stress state by an ultrasonic time-of-flight technique, *Insight*, **40**, 421-428, 1996

[5] I. Verpoest, E. Aernoudt, A. Deruyttere & M. Neyrinck, An improved ACPD method for detecting surface microcracks during fatigue tests of unnotched specimens, *Fatigue of Engineering Materials and Structures*, **3**, 203-217, 1980

[6] Y. Nakai & R.P. Wei, Measurement of short crack lengths by an AC potential method, *Engineering Fracture Mechanics*, **32**, 581-589, 1989

[7] G.P. Gibson, Evaluation of the AC potential drop method to determine J-crack resistance curves for a pressure vessel steel, *Engineering Fracture Mechanics*, **32**, 387-401, 1989

[8] T.V. Venkatasubramanian & B.A. Unvala, An AC potential drop system for monitoring crack length, *Journal of Physics E: Sci. Instrum.*, **17**, 765-771, 1984

[9] J.A. Joyce & C.S. Schneider, Crack length measurement during rapid crack growth using an ACPD method, *Journal of Testing and Evaluation*, **16**, 257-270, 1988

[10] I.S. Hwang & R.G. Ballinger, A multi-frequency AC potential drop technique for the detection of small cracks, *Meas. Sci. Technol.*, **3**, 62-74, 1992

[11]A.K. Soh & L.C. Bian, Mixed mode fatigue crack growth criteria, *International Journal of Fatigue*, **23**, 427-439, 2001

[12] D.A. Green, J.M. Kendall & J.F. Knott, Analytic and analogue techniques for determining potential distributions around angled cracks, **37**, R3-R12, 1988

[13] J. H. Lee, M. Saka & H. Abe, Loading Effect on ACPD of a Crack in Ferromagnetic Material, *Experimental Mechanics*, **37**, 32 – 136, 1997

[14] J. Zhou, J & A.M. Lewis, Thin-skin electromagnetic fields around a rectangular conductor bar, *Journal of Physics D: Applied Physics*, **26**, 1817-1823, 1993

[15] H. Cost, V. Deutsch, P. Ettel & M. Platte-Wuppertal, Crack depth measurement-Modern measuring technique for a well-known method, *NDTnet*, **1**, 1996

[16] S. Chen & P.B. Nagy, Edge weld penetration assessment using the potential drop technique, *NDT&E International*, **31**, 1-10, 1998

Volume 31, Issue 1, February 1998, Pages 1-10

[17] H.G. Beom, Small scale nonlinear analysis of electrostrictive crack problems, *Journal of the Mechanics and Physics of Solids*, **47**, 1379-1395, 1999

[18] C.P. You & J.F. Knott, *Engineering Fracture Mechanics*, **24**, 291-305, 1986